NASA TN D-927

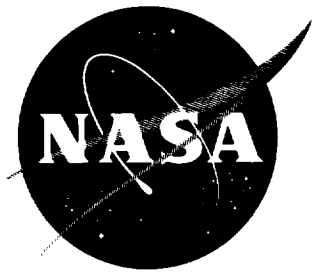

TECHNICAL NOTE

D-927

FREE-FLIGHT INVESTIGATION OF RADIO-CONTROLLED MODELS WITH PARAWINGS

By Donald E. Hewes

Langley Research Center
Langley Field, Va.

NATIONAL AERONAUTICS AND SPACE ADMINISTRATION

WASHINGTON September 1961

NATIONAL AERONAUTICS AND SPACE ADMINISTRATION

TECHNICAL NOTE D-927

FREE-FLIGHT INVESTIGATION OF RADIO-CONTROLLED MODELS WITH PARAWINGS

By Donald E. Hewes

SUMMARY

A free-flight investigation of two radio-controlled models with parawings, a glider configuration and an airplane (powered) configuration, was made to evaluate the performance, stability, and methods of controlling parawing vehicles. The flight tests showed that the models were stable and could be controlled either by shifting the center of gravity or by using conventional elevator and rudder control surfaces. Static wind-tunnel force-test data were also obtained.

INTRODUCTION

A free-flight investigation of two radio-controlled models with parawings has been made as part of an overall study being conducted by the Langley Research Center to determine the feasibility of several applications for the parawing described in reference 1. The present parawing consists of a fabric material cut to a 45° sweptback modified delta planform and attached to three structural members all joined at one end to form the leading edges and the root chord, or keel, of this wing. Use of a pivoted or flexible joint at the nose of the wing allows the sweepback angle to vary with varying air loads and also permits the wing to be collapsed or folded into a small space. The relatively light weight and the folding capability of this type of construction make this wing quite attractive for several applications. References 1 to 3 present results of wind-tunnel tests and some uncontrolled flight tests of parawing gliders and illustrate the uses of this parawing as a high-lift device for landing aircraft and as a recovery system for manned space vehicles.

The present investigation was made with free-flying dynamic models to evaluate qualitatively the performance, stability, and methods for controlling vehicles incorporating the parawing. One method of control was to shift the center of gravity of the vehicle fore and aft for pitch control and side to side for roll or lateral control. The model used to study this method of control was a glider launched from a helicopter and consisted of a fuselage suspended below the parawing by

a system of cables (fig. 1); the radio-control equipment and motion-picture camera were housed within the fuselage. Shifting the center of gravity of this model was achieved by changing the lengths of the suspension cables or lines. The other method of control employed conventional tail surfaces and rudder and elevator control. The flight test model, herein referred to as the airplane model, used to study this method of control consisted of the fuselage and tail surfaces of a small powered target drone trainer and the parawing supported by a rigid pylon attached to the fuselage. (See fig. 2.) In addition to the flight tests, some wind-tunnel static force tests of the airplane model and also of a rigid metal wing (fig. 3) were made to determine some aerodynamic characteristics; the rigid wing, which simulated the flexible parawing, was tested with three different angles of leading-edge sweep: 45°, 50°, and 60°.

SYMBOLS

All forces and moments, with the exception of lift and drag, are presented with respect to a system of body axes originating at a specific reference point. In the case of the rigid-wing force tests, the reference point was located at the reference center of the balance and the body axes were alined with respect to the keel of the wing (fig. 4); whereas, for the force tests of the airplane model, the reference point was the flight center-of-gravity location of the model and the axes were alined with the thrust axes (fig. 5).

In order to facilitate the comparison of data, all coefficients regardless of the sweepback angle of the wing were based on the area, span, and mean aerodynamic chord of the flat planform of the parawing - that is, the wing with 45° sweepback.

b	wing span (based on flat planform), ft
$\bar{c}$	mean aerodynamic chord (assumed in plane of leading edges and keel), ft
q	dynamic pressure, $\frac{1}{2}\rho V^2$, lb/sq ft
S	wing area (based on flat planform), sq ft
V	free-stream velocity, ft/sec
W	weight, lb
X,Y,Z	body reference axes

x,z	distance along X- and Z-axis, respectively, positive forward and downward, ft
α	angle of attack, deg
β	angle of sideslip, deg
Δl	ratio of linear travel of lateral-control suspension lines to mean aerodynamic chord
Δm	ratio of linear travel of longitudinal-control suspension lines to mean aerodynamic chord
Δx	ratio of longitudinal displacement of center of gravity to mean aerodynamic chord
Δy	ratio of lateral displacement of center of gravity to mean aerodynamic chord
Δz	ratio of vertical displacement of center of gravity to mean aerodynamic chord
δ_e	deflection of elevator, positive with trailing edge down, deg
δ_r	deflection of rudder, positive with trailing edge to left, deg
ρ	mass density of air, slugs/cu ft
F_D,D	drag, lb
F_L,L	lift, lb
F_Y	side force, lb
M_X	rolling moment, ft-lb
M_Y	pitching moment, ft-lb
M_Z	yawing moment, ft-lb
C_D	drag coefficient, F_D/qS
C_L	lift coefficient, F_L/qS
C_l	rolling-moment coefficient, M_X/qSb

C_m pitching-moment coefficient, $M_Y/qS\bar{c}$

C_n yawing-moment coefficient, M_Z/qSb

$C_X = -\left(C_D \cos \alpha - C_L \sin \alpha\right)$

C_Y side-force coefficient, F_Y/qS

$C_Z = -\left(C_D \sin \alpha + C_L \cos \alpha\right)$

$C_{L_\alpha} = \frac{\partial C_L}{\partial \alpha}$ per degree

$C_{m_\alpha} = \frac{\partial C_m}{\partial \alpha}$ per degree

$C_{X_\alpha} = \frac{\partial C_X}{\partial \alpha}$ per degree

$C_{Z_\alpha} = \frac{\partial C_Z}{\partial \alpha}$ per degree

$C_{l_\beta} = \frac{\partial C_l}{\partial \beta}$ per degree

$C_{n_\beta} = \frac{\partial C_n}{\partial \beta}$ per degree

$C_{Y_\beta} = \frac{\partial C_Y}{\partial \beta}$ per degree

$C_{m_{\delta_e}} = \frac{\partial C_m}{\partial \delta_e}$ per degree

Subscript:

max maximum

MODELS AND TEST EQUIPMENT

Rigid-Wing Model

The rigid-wing model used to simulate the parawing for the static force tests was constructed of 3/8-inch-diameter steel tubing 2.5 feet

in length and covered with 0.016-inch sheet aluminum in place of the fabric. (See figs. 3 and 4.) The sheet-metal covering was shaped to represent the contours which would be assumed by the fabric for three different angles of sweepback of the leading edges. The sweepback of the model was changed by bending the leading-edge tubes at the nose joint. Nose cant, which had been shown in some unpublished test results to be useful in achieving satisfactory deployment of flexible-wing models, was provided for some of the tests by bending all three tubes about 4 inches from the nose and refitting the sheet-metal covering at the nose. A strain-gage balance to measure all force and moment components was attached to the wing by means of two tubular braces which supported the wing about 0.75 foot above the balance. (See fig. 4.)

Radio-Controlled Glider Model

Details of the radio-controlled glider are shown in figures 1, 6, 7, 8, and 9; the pertinent physical characteristics are given in table I. The planform of the parawing of the glider model was the same as that of the rigid wing. The wing keel and leading edges were 6.0 feet in length and were constructed of 3/4-inch hardened aluminum tubing 5.0 feet in length joined to a foldable nose assembly. The nose assembly used initially consisted of three narrow flat strips of spring steel joined together rigidly at one end and each joined at the other end to one of the pieces of tubing. A photograph of the glider model with parawing, hereinafter referred to as the original model, is shown as figure 1. Bending of these spring-steel strips provided the means for folding the parawing to facilitate mounting of the glider to the launch helicopter. For most of the tests, however, this assembly was replaced with a unit constructed mainly of 3/4-inch steel tubing with a toggle joint (fig. 7) which permitted the wing to be folded and also to be locked with the leading edges at about 54° sweepback in the fully deployed condition during flight. This configuration is referred to as the modified model (fig. 8). The tubular frame was covered with parachute nylon bonded to a 1/4-mil-thick Mylar film used to seal the porous fabric. The wing was connected to the fuselage by two suspension lines attached to each of the wing structural members.

The fuselage of the glider was constructed of molded fiber-glass-reenforced plastic and contained an 8-mm electrically driven motion-picture camera, a four-channel radio-control receiver, two control actuators and linkages, and a battery power supply. A photograph of the control actuators installed in the modified model is shown in figure 9. The actuators operated two control arms which were rotated from the neutral positions in either direction with a flicker or bang-bang action in response to radio-control signals. On the original model, the suspension lines from the wing keel (used for pitch control) and from the leading edges (used for roll control) were attached directly to the

control arms. Movement of the arms caused the fuselage to rotate relative to the wing and displace the fuselage center of gravity to achieve longitudinal and lateral control. For the modified model, the suspension lines attached to the keel were passed through a guide, referred to as the suspension point, at the top and on the center line of the fuselage. Also, for the modified model, the suspension lines attached to the wing leading edges were passed through guides displaced 4 inches laterally from the suspension point. Movement of the control arms for this arrangement changed the effective lengths of the lines and resulted in greater movement of the center of gravity for the same amount of control-arm travel than was obtained with the original model.

A nose boom was attached to the fuselage in view of the motion-picture camera. This boom supported a flow-direction vane, which indicated angles of attack and sideslip of the fuselage, and two movable pointers, which indicated the movement and position of the control actuators. The camera also recorded the view of the horizon and surrounding terrain to facilitate the qualitative evaluation of the motions of the model. A metal tail boom with two stabilizing fins was attached to the rear of the fuselage to keep it alined with the direction of flight. Total weight of the model was 23.5 pounds including 5.0 pounds for the wing.

Radio-Controlled Airplane Model

Details of the radio-controlled airplane model using the flexible wing as the main lifting surface are shown in figures 2 and 5; the pertinent physical characteristics are given in table II. The wing was the same size and construction as that for the glider except that the foldable nose assembly was replaced by a rigid nose which held the leading edges fixed at about 50° sweepback. A tubular pylon was used to support the wing, and cables were used to restrain the wing from rotating relative to the fuselage. An internal combustion engine with a maximum rating of about 1 horsepower was installed in the model. A conventional landing gear was provided to permit the evaluation of the take-off and landing characteristics of the airplane. The total weight of the airplane was 15.5 pounds.

Control of the airplane was provided by conventional rudder and elevator surfaces which could be deflected about ±20°. The rudder was operated in either direction from the neutral position with a flicker or bang-bang action in response to radio control signals. The elevator moved slowly between the full-up and full-down limits in response to the radio signals. When the signals were stopped, the elevator remained in its last position.

TESTS

Static wind-tunnel force tests of the rigid-wing model and the airplane model were made in the 12-foot low-speed tunnel located at the Langley Research Center. Tests of the rigid wing alone were made for ranges of angle of attack from 0° to 50° and of sideslip angle from 0° to ±15° for sweepback angles of 45°, 50°, and 60° at a dynamic pressure of 4.7 pounds per square foot and a Reynolds number of about 400,000 per foot or 670,000 based on the mean aerodynamic chord. Tests of the airplane model were made for ranges of angles of attack from 0° to 28° and of sideslip angle from 0° to ±15°, mostly at a dynamic pressure of 2.3 pounds per square foot and a Reynolds number of about 281,000 per foot. A few additional lateral force tests at the higher angles were made at a lower dynamic pressure of 1.6 pounds per square foot because of excessive lateral loads on the model structure.

Flight tests of the glider were made by launching the model from the helicopter at an airspeed of about 20 knots, which was close to the airspeed for $(L/D)_{max}$ of the glider or minimum glide-path angle, and at an attitude of about 1,100 feet which permitted about 2 minutes of flight time. The tests consisted of a series of glides in which both longitudinal and lateral controls were operated to fly the model through desired flight maneuvers. These tests were made with the suspension point of the fuselage located at various fore and aft positions relative to the keel of the wing but at only one vertical position, about $0.77\bar{c}$ below the keel. Motion-picture records were taken from the helicopter, from the ground, and from the model.

The flight tests of the airplane consisted of a series of take-offs, low-altitude flights, and landings to obtain a qualitative evaluation of the ground handling qualities and the stability and control characteristics of the vehicle in flight. The flights were made from a concrete runway in winds with velocities ranging from about 5 to 15 knots.

For both series of flight tests, the models were flown by an operator at a ground station located within visual range of the model, generally within 1,000 feet.

RESULTS AND DISCUSSION

The results of the static longitudinal and lateral force tests of the rigid-wing model are presented in figures 10 and 11, respectively. The force-test data for the airplane model are presented in figures 12 and 13. Motion-picture records of the flight tests of the glider and

airplane models are presented in a film supplement to this report, which is available on loan. A request card form and a description of the film will be found at the back of this paper on the page immediately preceding the abstract pages.

Static Force Tests of Rigid-Wing Model

The tests of the rigid-wing model, which simulated the flexible parawing with different angles of sweepback, were made as an expedient means to evaluate some of the effects of leading-edge flexing on the aerodynamic characteristics. Caution should be exercised in attempting to apply these particular data directly to actual parawing applications since the simulation may be rather poor for some conditions where flexibility is important. It is believed, however, that the simulation is adequate for the particular effects to be studied.

Longitudinal stability and control.- The variations of lift, drag, pitching moment, and lift-drag ratio with angle of attack (fig. 10) for sweepback angles of 45°, 50°, and 60° of the rigid wing indicate that a maximum lift coefficient of 1.15, a lift-curve slope of about 0.048 per degree, and a maximum lift-drag ratio of 7.7 were obtained. The maximum lift-drag ratio obtained for the 50° sweptback wing occurred at an angle of attack of about 22° and a lift coefficient of 0.53. The value of $(L/D)_{max}$ was reduced by about 40 percent as the sweepback angle was increased from 50° to 60°; a further reduction resulted from canting (bending) the nose up 15°.

There was a marked effect of sweep angle on the lift and drag of the rigid wing for a given angle of attack. Although the lift-curve slope C_{L_α} and maximum lift were affected to some extent, the primary effect was to shift the angles of attack for zero lift and minimum drag to larger values as the sweep angle increased. This shift is attributed to the variation of the surface contour with sweep angle, and an approximate measure of this angle-of-attack increment is the projected angle between the reference chord plane (that is, the plane of the leading edges and keel) and the upper surface of the wing as seen in the sideview of the wing. (See fig. 4.)

Changing the sweep angle from 45° to 50° produced a large stabilizing change in the pitching moment but further increasing the sweep angle produced only a relatively small stabilizing change (fig. 10). Bending or canting the nose up 15° had practically no effect on trim and had a small destabilizing effect on the longitudinal stability.

Lateral stability and control.- In general, the data from the lateral force tests indicated linear variations of the side force and the rolling

and yawing moments with sideslip angle. The results of these tests are summarized in figure 11 which shows the variations of the slopes of these data curves measured at zero sideslip angle with angle of attack. There was generally a marked increase of the lateral static stability with sweep angle. Inasmuch as C_{n_β} with respect to the body axes is not a direct measure of the directional stability, the corresponding values for C_{n_β} relative to the stability axes (which is the direct measure of directional stability) are given in this figure for the 50° sweep angle. The curves for these values of C_{n_β} show that increasing the angle of attack did not seriously affect the directional stability, at least for the range of the tests.

Interpretation of the test data.- Considering the effects of sweep angle on the lift-drag ratio and on longitudinal and directional stability, it appears that there is an optimum sweep angle of about 50° for the rigid wing. For the lower sweep angle the stability was reduced, and for the higher angle the lift-drag ratio or performance was decreased. On the basis of these results for the rigid wing, it is believed that a corresponding optimum sweep angle exists for a parawing utilizing a fabric surface. If this assumption is correct and optimum performance is desired, the wing structure and rigging should be designed to maintain approximately a 50° leading-edge sweep angle for the particular combination of flight conditions to be encountered. In cases where the flight conditions will vary appreciably during a given flight, it may be desirable to make the structure as stiff as possible in order to maintain the optimum sweep angle. Of course, some practical compromise will be required because of the added weight involved to produce stiffness. In order to evaluate the particular structural requirements for a flexible parawing, more extensive tests must be made with a flexible model under conditions simulating as closely as possible actual flight.

Static Force Tests of Airplane Model

Longitudinal stability and control.- The variations of lift, drag, pitching moment, and lift-drag ratio with angle of attack for the airplane model given in figure 12 indicate a maximum lift coefficient of about 1.05, a lift-curve slope of approximately 0.044 per degree, and a maximum lift-drag ratio of 4.4 for the complete model and of 6.2 for the airplane wing alone. The lift characteristics of the fabric-covered wing (50° sweepback angle) agree fairly well with those for the rigid-wing model for the same sweep angle $\left(C_{L,max} = 1.15 \text{ and } C_{L_\alpha} = 0.048\right)$. The lower lift-drag ratio of the fabric-covered wing as compared with the lift-drag ratio of the metal wing is attributed mainly to the added drag of the pylon and cables used to support the wing on the balance and also to the rather poor surface condition of the fabric. It was observed that the

fabric was free of fluttering for angles of attack of the model above about 8° (corresponds to about 23° for the wing) which is slightly less than the angle of attack for $(L/D)_{max}$. As the angle of attack was decreased below 8°, however, fluttering, which appeared to be similar to the waving action of a flag in a stiff breeze, was evident over portions of the wing surface. The model was longitudinally stable with a value of C_{m_α} of -0.0046 or a static margin $\partial C_M/\partial C_L$ of -0.10$\bar{c}$ and a value of elevator effectiveness parameter $C_{m_{\delta_e}}$ of about -0.0015 per degree throughout the test angle-of-attack range.

Lateral-directional stability and control.- In general, the data from the lateral force tests indicated linear variations of the side force and the rolling and yawing moments with sideslip. The results of these tests are summarized in figure 13, which shows the variations of the slopes of these data curves at zero sideslip angle with angle of attack, and indicate effective dihedral and directional stability for the airplane model over the test angle-of-attack range.

L 13 74

Flight Tests of Glider Model

As stated previously, the flight tests were aimed principally at evaluating qualitatively the stability of the glider model and determining the feasibility of shifting the center of gravity as a means of control. Evaluation of the flight characteristics was based solely on the opinion of the control operators and observers. The data consist primarily of motion-picture records of several flights, which are included in the film supplement to this report.

Model modifications.- During the attempts to fly the original glider model which incorporated the wing-flexible-nose assembly, it was found that, although the model was stable and controllable, the wing leading edges attained excessive sweepback angles (greater than 60°). These angles were considered to be detrimental to the gliding performance on the basis of the force-test results for the rigid-wing model. In earlier preliminary tests of the parawing, in which uncontrolled glider models with the same type of nose construction were used, satisfactory results had been obtained (ref. 1). The wing loadings for these early tests, however, were relatively light - that is, of the order of 0.25 to 0.50 pound per square foot as compared with 0.93 pound per square foot for the present tests. It was thought, therefore, that because of the heavier wing loading the flexible nose would have to be replaced with a unit providing greater stiffness in order to achieve the best gliding characteristics of the model. Most of the tests were made with the stiffer nose unit which locked the leading edges at an angle of sweepback of about 54°.

A further modification was a change in the attachment of the suspension lines to the model. Flight tests of the original model in which the lines were attached directly to the control arms indicated relatively weak control response. Consequently, the suspension lines were passed through a guide at the top of the fuselage to improve the control response by increasing the center-of-gravity travel for the fixed amount of control-arm travel available.

As the test program progressed, the surface condition of the wing deteriorated due to handling and damage sustained in landing. The poor condition of the fabric caused the wing contours to be uneven and wrinkled; although this condition caused the fabric to flutter during flight, the flight characteristics in general did not appear to be adversely affected.

Only the modified model is considered in the following discussion.

Longitudinal stability and control.- During the tests, the suspension point of the fuselage was varied relative to the keel of the wing from about $0.55\bar{c}$ to $0.77\bar{c}$ aft of the leading edge of $\bar{c}$ and at a distance of about $0.77\bar{c}$ below the wing keel by movement of the control arm and, also, by adjustment of the lengths of the fore and aft suspension lines between flights. The corresponding locations of the center of gravity of the model were considered to be between about $0.48\bar{c}$ and $0.61\bar{c}$ aft and at about $0.64\bar{c}$ below, based on the simplifying assumptions that the wing and lines were rigid during flight and that the weight of the fuselage was concentrated at the suspension point. The center of gravity of the wing alone was located at about $0.16\bar{c}$ aft of the leading edge of $\bar{c}$.

The model was longitudinally stable over the center-of-gravity range of the tests, except at the most rearward position where a divergent longitudinal oscillation with a period of 2 to 3 seconds was encountered as the model stalled. This oscillation required several cycles to build up to the point where the model tumbled, and recovery from the oscillation prior to the tumbling motion could be achieved merely by shifting the center of gravity forward. At the most forward position the model glided in a relatively steep dive and the wing fabric fluttered with an action similar to that noted in the force tests of the airplane wing for angles of attack somewhat below that for $(L/D)_{max}$.

The best gliding characteristics of the model were obtained with the suspension point located at about $0.60\bar{c}$ aft of the leading edge of $\bar{c}$ which corresponds to about $0.53\bar{c}$ aft for the center of gravity. On the basis of measurements of the airspeed determined by using the helicopter to pace the model, the lift coefficient for this condition of $(L/D)_{max}$ was estimated to be between 0.5 and 0.6.

The pitch control system for the modified model provided initially about $\pm 0.03\bar{c}$ fore-and-aft movement of the center of gravity from the

neutral control position. The opinion of the operator controlling the model was that this movement was not sufficient to achieve the desired maneuvering capability particularly for flaring the model on landing. The system was subsequently modified by doubling the length of the pitch control arm to provide about $\pm 0.06\bar{c}$ movement which appeared to be adequate.

Analysis of longitudinal stability and control.- Inasmuch as the flight tests were made with the center of gravity located essentially at only one vertical position below the wing and at several horizontal positions, an analysis was made to determine the effect of shifting the center of gravity in both directions on the stability and control of the glider. The analysis was based on equations derived simply from the moment transfer equation:

$$(C_m)_2 = (C_m)_1 + \Delta x C_Z - \Delta z C_X \tag{1}$$

where $(C_m)_1$ is the pitching moment about some reference point and $(C_m)_2$ is the moment acting about a point located at distances Δx and Δz from the reference point. The following equation was used to determine the combinations of Δx and Δz which produce a condition of trim - that is, $(C_m)_2 = 0$ - at a given lift coefficient:

$$\Delta x = \Delta z \frac{C_X}{C_Z} - \frac{(C_m)_1}{C_Z} \tag{2}$$

where C_X, C_Z, and $(C_m)_1$ are known values for the given lift coefficient. To obtain the combinations of Δx and Δz which produce a constant value of C_{m_α}, equation (1) was differentiated and rearranged to give the following expression:

$$\Delta x = \Delta z \frac{C_{X_\alpha}}{C_{Z_\alpha}} - \frac{(C_{m_\alpha})_1 - (C_{m_\alpha})_2}{C_{Z_\alpha}} \tag{3}$$

where C_{X_α}, C_{Z_α}, and $(C_{m_\alpha})_1$ are known values for the given lift coefficient and $(C_{m_\alpha})_2$ is set equal to the desired value - in this case,

0 or -0.005 which corresponds to neutral stability and to a static margin of $0.10\bar{c}$, respectively. Since no force-test data were available for the airplane model, the values for the aerodynamic terms were approximated by using the data for the rigid-wing model with 50° sweepback angle and by neglecting the drag of the fuselage and suspension lines. The errors resulting from these assumptions are believed to be relatively small as far as general trends are concerned.

The results of this analysis are presented in figure 14 which shows the combinations of $\frac{x}{\bar{c}}$ and $\frac{z}{\bar{c}}$, with respect to the mean aerodynamic chord, which produce longitudinal trim $\left((C_m)_2 = 0\right)$ and values of C_{m_α} of 0 and -0.005 for values of C_L of 0.40, 0.53 $\left((L/D)_{max}\right)$, and 0.80. The reference point for the measured aerodynamic data and also the ranges for the suspension-point and center-of-gravity locations tested in flight are shown in this figure. The figure indicates that both longitudinal stability and trim can be achieved for any vertical location lower than $0.10\bar{c}$ below the wing and that the stability is increased for a given trimmed lift coefficient as the center of gravity is lowered. The amount of center-of-gravity shift required to produce a given change in trim increases correspondingly as the center of gravity is lowered. It is interesting to note that longitudinal control can be achieved by shifting the center of gravity either horizontally or vertically. The fact that the center of gravity of the model for best glide $\left(\frac{x}{\bar{c}} = 0.53 \text{ at } \frac{z}{\bar{c}} = 0.64\right)$ did not coincide with the curve for $C_L = 0.53$ $\left((L/D)_{max}\right.$ for the rigid wing$\left.\right)$ is attributed to the errors introduced by the assumptions previously discussed. On the basis of these results (fig. 14), it appears that satisfactory longitudinal stability and control could have been maintained with the suspension lines shortened appreciably from the lengths used in the tests.

Lateral-directional stability and control.- The model appeared to be laterally and directionally stable for the range of test center-of-gravity positions. Oscillations induced by gust or control applications appeared to be heavily damped. At the stall, the model showed no serious roll-off or directional divergent tendencies.

The roll control system provided about $\pm 0.06\bar{c}$ lateral shift of the center of gravity which was sufficient to produce the desired maneuvering capability for most of the fore-and-aft center-of-gravity test range. At the most forward position where a large portion of the wing fabric fluttered, effectiveness of the lateral control was noticeably reduced.

For most of the tests, application of roll control was accompanied by a yawing of the fuselage relative to the wing. This yawing was

attributed to the action of the lateral suspension lines on the line guides which were 4 inches from the center line of the fuselage. Although the yawing resulted in as much as 10^{C} to 20^{O} difference between wing and fuselage, the response of the model to roll control did not appear to be adversely affected. A few flights were made with the lines passing through the guide at the center line of the fuselage and this yawing due to roll control was virtually eliminated.

Landing characteristics.- Because of the relatively low value of $(L/D)_{max}$ of this model (estimated to be in the order of 4 to 5) and limitations of the bang-bang type of control system employed, some difficulty was experienced in performing satisfactory landings. By employing a landing technique in which the approach was made at a speed higher than that for $(L/D)_{max}$ and then increasing angle of attack just prior to touchdown to execute the flare, a few successful landings were made. Relatively little difficulty was experienced in maneuvering the model laterally to maintain the desired glide path during these landings. L 1 3 7 4

After touchdown of the fuselage, the wing was observed to maintain lift momentarily and then drop down on top of and slightly ahead of the fuselage. On one landing in which the flare was initiated too late, the wing pitched up, rolled to the left, and pulled the fuselage back into the air in a banked turn. No provisions were made to disconnect the wing from the model at touchdown.

On the basis of the demonstrated flare capability of the parawing-equipped model and the experience gained with landing this model, it is believed that precise remotely controlled landings can be made by employing a proportional control system in place of the present system and also by providing two control operators. One operator should be located at the end of the landing path to provide lateral control and the other, to one side of the landing path to observe the altitude and pitch attitude and provide pitch control. Some means should be employed to disconnect the wing at touchdown to help prevent entanglement of the wing and fuselage during the ground runout.

Flight Tests of Airplane Model

As previously stated, the purpose of these tests was to evaluate qualitatively the stability of the airplane model and determine the feasibility of using only the conventional type of tail surfaces for control. Evaluation of the flight characteristics was based solely on the opinion of the control operator and observers. The data consist primarily of motion-picture records of several flights, which are included in the film supplement to this report.

Take-off and landing characteristics.- Limited ground-taxi and take-off tests showed that the model could be maneuvered satisfactorily with the rudder except in cross winds. When encountering a cross wind during take-off, the model would pick up the wing on the windward side and turn downwind due to the effective dihedral of the model and lack of roll control. Results of tests made with a similar configuration using a cross-wind landing gear which permitted the model to yaw into the wind during take-off indicated that this problem was alleviated.

Longitudinal stability and control.- All tests were made with the center of gravity located $0.46\bar{c}$ aft and $0.33\bar{c}$ below the leading edge of $\bar{c}$, and for this location the model was longitudinally stable during take-off, level and turning flight, and landing. At the stall, the model pitched down gently without experiencing divergent longitudinal oscillations.

The elevator was effective as a means for controlling the model in pitch although some difficulty was experienced in controlling the model. It is believed that this result was due to the trimming type of elevator control system, used as a simple expedient for these exploratory tests, rather than to the response characteristics of the model. With some practice in anticipating the motion of the model to overcome the control lag introduced by this system, the operator could control the model effectively. Either a trimmable bang-bang type of control or a proportional-type control is recommended as a practical replacement for this unsatisfactory elevator control system.

Lateral stability and control.- In level flight at an estimated lift coefficient of about 0.6, the airplane model was stable laterally and directionally and could be maneuvered effectively by using the rudder as the only means for lateral control. Oscillations induced by gust or control applications appeared to be heavily damped. There were no serious roll-off or directional divergent motions as the model entered the stall and pitched down gently.

CONCLUDING REMARKS

In general, the flight tests showed that the radio-controlled models with parawings - a glider configuration and an airplane (powered) configuration - were stable and could be controlled either by shifting the center of gravity or by using conventional elevator and rudder control surfaces. Results indicated the desirability of providing as much stiffness as practical for the nose structure of the parawing in order to maintain the optimum leading-edge sweep angle (approximately 50°) for maximum performance under varying flight conditions. Wind-tunnel static

force tests indicated that lift coefficients greater than 1.0 and a maximum lift-drag ratio greater than 4.5 can be attained with the parawing.

Langley Research Center,
National Aeronautics and Space Administration,
Langley Field, Va., May 24, 1961.

REFERENCES

1. Rogallo, Francis M., Lowry, John G., Croom, Delwin R., and Taylor, Robert T.: Preliminary Investigation of a Paraglider. NASA TN D-443, 1960.

2. Rogallo, F. M., and Lowry, J. G.: Flexible Reentry Gliders. Preprint no. 175C, Soc. Automotive Eng., Apr. 1960.

3. Naeseth, Rodger L.: An Exploratory Study of a Parawing As a High-Lift Device for Aircraft. NASA TN D-629, 1960.

TABLE I.- PHYSICAL CHARACTERISTICS OF THE GLIDER MODEL

Total weight of glider model, lb	23.5
Parawing:	
Weight, lb	5.0
Area (total cloth), sq ft	25.4
Loading, W/S, lb/sq ft	0.93
Span, ft	8.48
Root chord, ft	6.0
Mean aerodynamic chord, ft	4.0
Sweepback angle, deg	(approx.) 54
Suspension line lengths from wing to suspension point at top of fuselage for best gliding characteristics:	
Front, ft	4.02
Rear, ft	3.60
Distance from wing to suspension point for best gliding characteristics:	
Vertical, percent $\bar{c}$	77
Horizontal (from leading edge of $\bar{c}$), percent $\bar{c}$	60
Fuselage:	
Width, ft	0.50
Length, ft	2.42
Depth, ft	0.75
Distance from fuselage nose to suspension point, ft	1.09
Vertical distance from suspension point to fuselage center of gravity, ft	0.63
Tail:	
Length (distance from fuselage center of gravity to 0.25$\bar{c}$ of tail surfaces), ft	2.09
Area, sq ft	0.55
Dihedral angle, deg	-45
Longitudinal control:	
Δm	$\pm$0.026 and 0.052
Δx	$\pm$0.03 and 0.06
Lateral control:	
Δl	$\pm$0.044
Δy	$\pm$0.06

TABLE II.- PHYSICAL CHARACTERISTICS OF AIRPLANE MODEL

Weight of airplane model, lb	15.5
Parawing:	
Area (total cloth), sq ft	25.4
Loading, W/S, lb/sq ft	0.61
Span, ft	8.48
Root chord, ft	6.0
Mean aerodynamic chord, ft	4.0
Sweepback angle, deg	(approx.) 50
Incidence angle, deg	15
Attachment point, percent $\bar{c}$	40
Attachment height above fuselage reference point, ft	1.56
Horizontal location of center of gravity (relative to wing), percent $\bar{c}$	46
Vertical location of center of gravity (relative to wing), percent $\bar{c}$	33
Fuselage:	
Length, ft	5.0
Depth, ft	0.54
Width, ft	0.46
Horizontal tail:	
Length, ft	3.20
Area, sq ft	0.24
Elevator deflection, δ_e, deg	±20
Vertical tail:	
Area, sq ft	0.65
Rudder area, sq ft	0.21
Rudder deflection, δ_r, deg	±20

L-60-1459

Figure 1.- Radio-controlled glider model with the original parawing and suspension system.

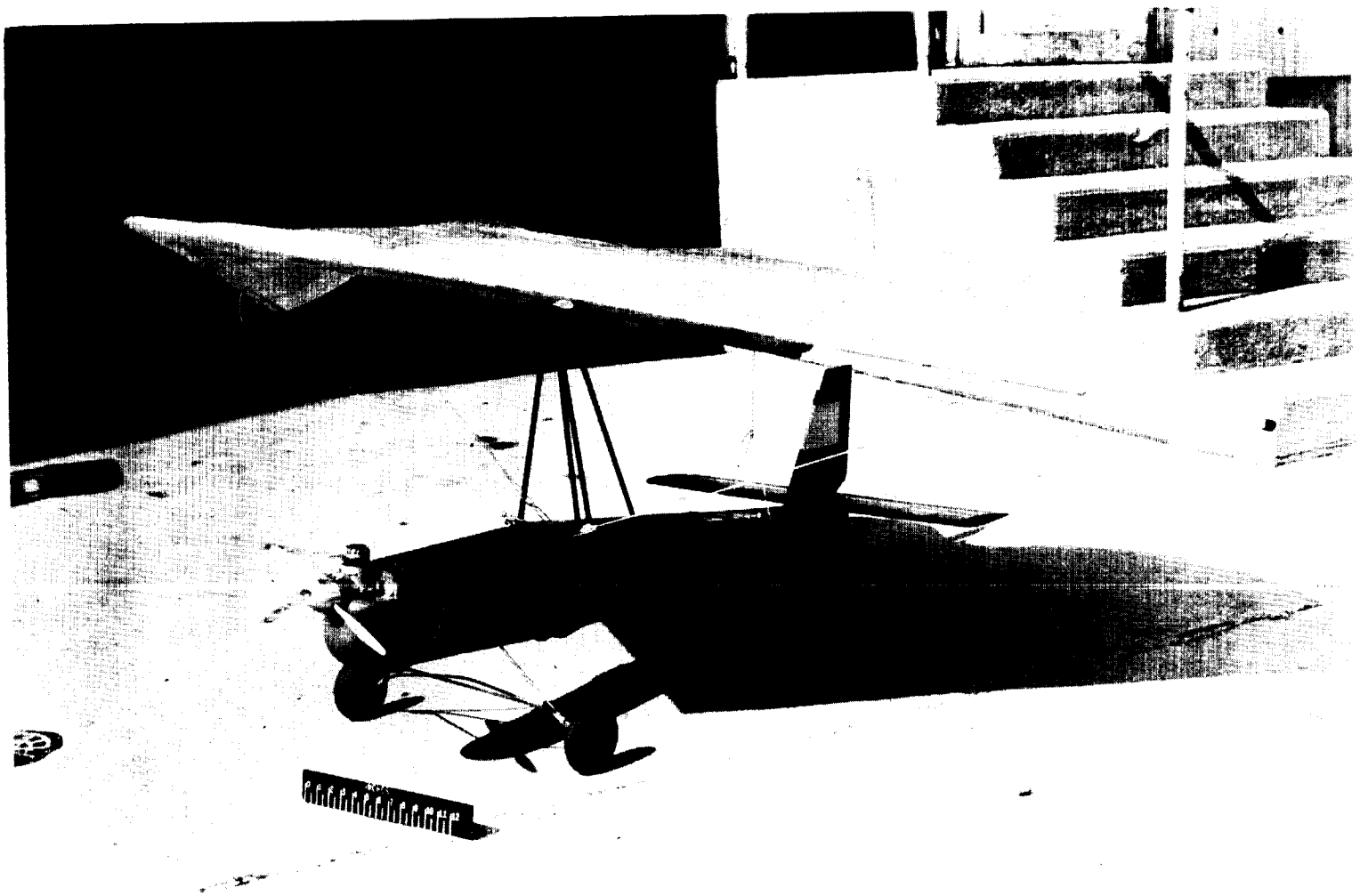

Figure 2.- Radio-controlled airplane model with parawing. L-60-3017

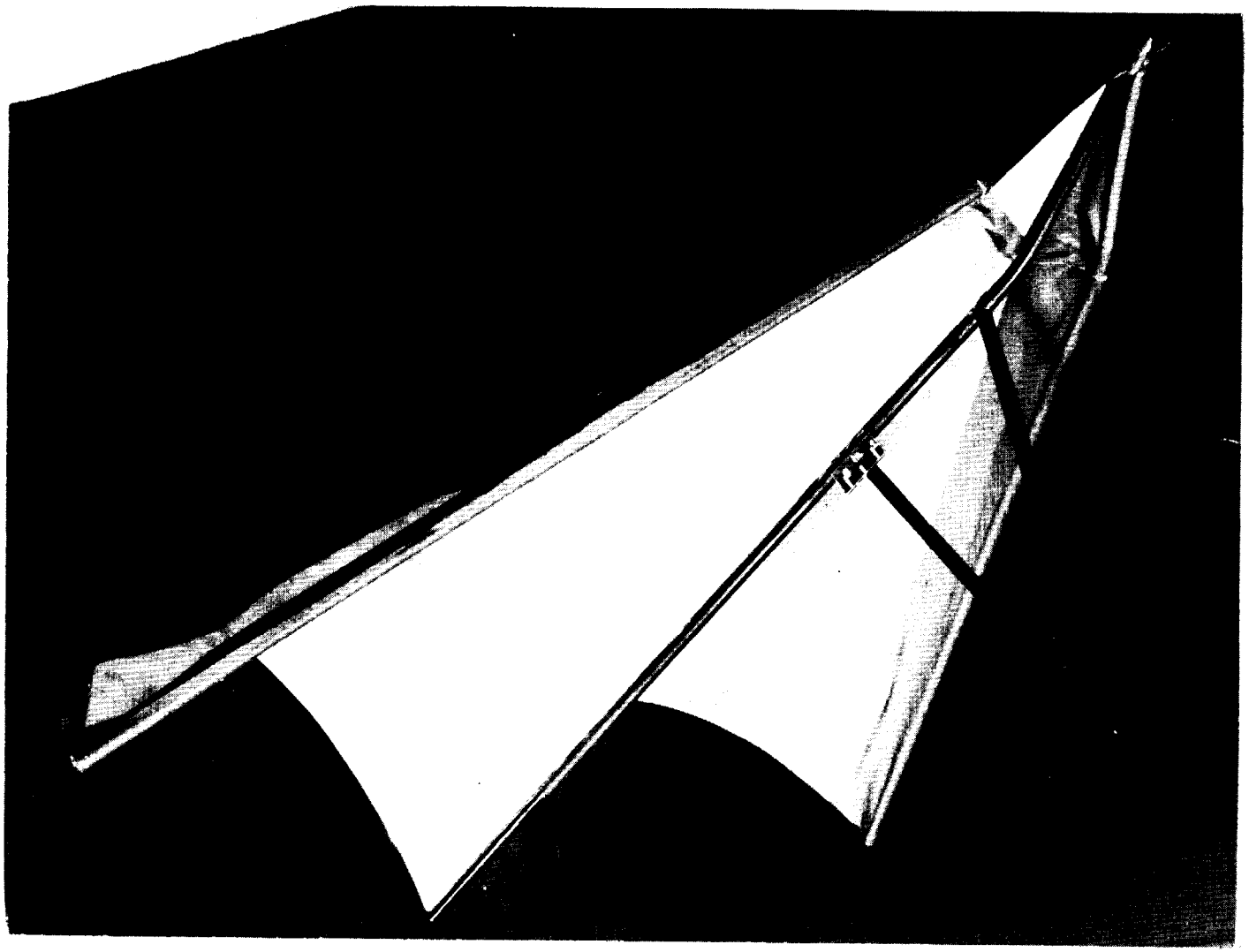

Figure 3.- Rigid-wing force-test model with 60° sweepback and canted nose. L-60-5967

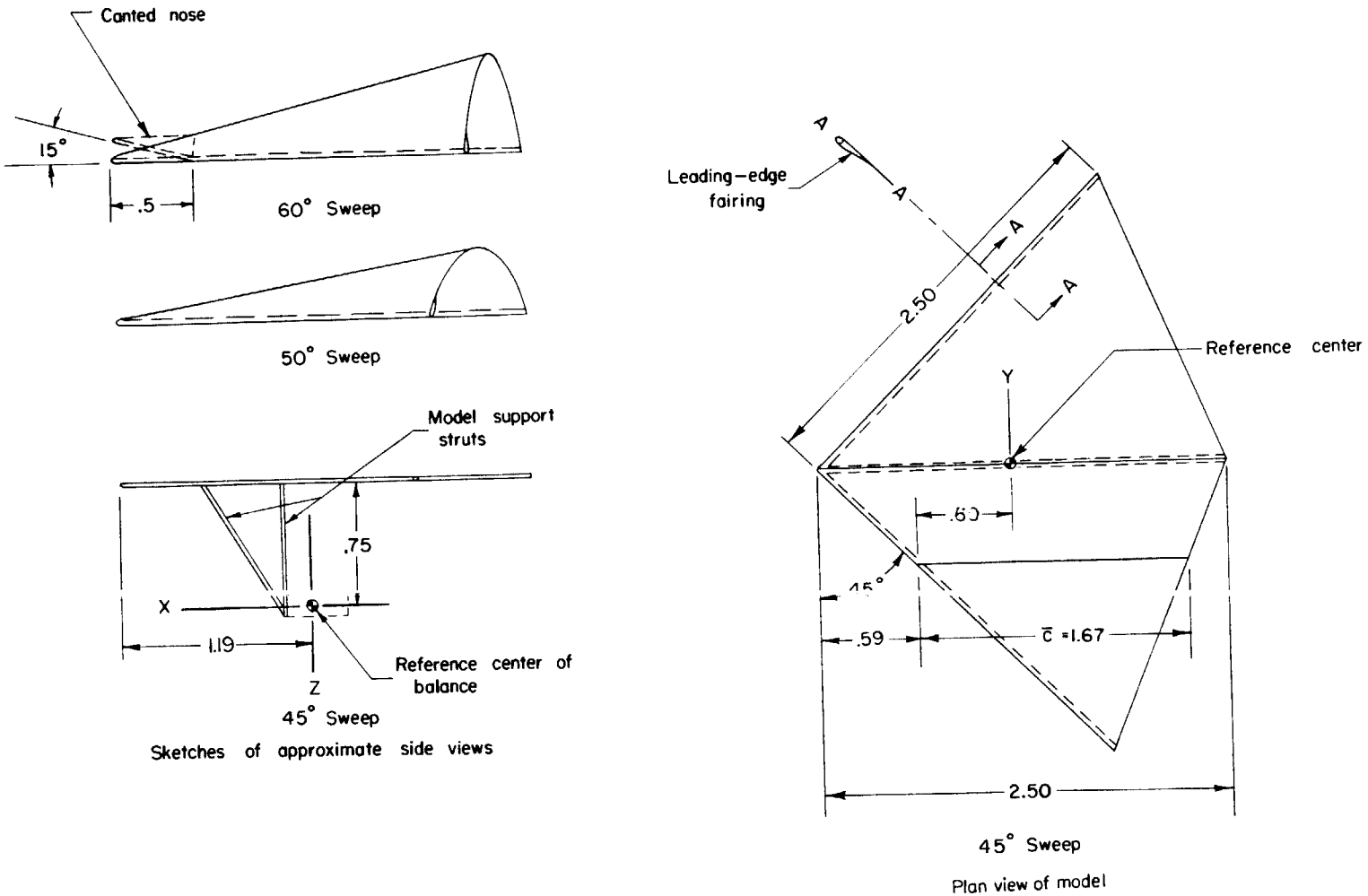

Figure 4.- Sketch of rigid wing used in wind-tunnel static force tests. All linear dimensions are in feet.

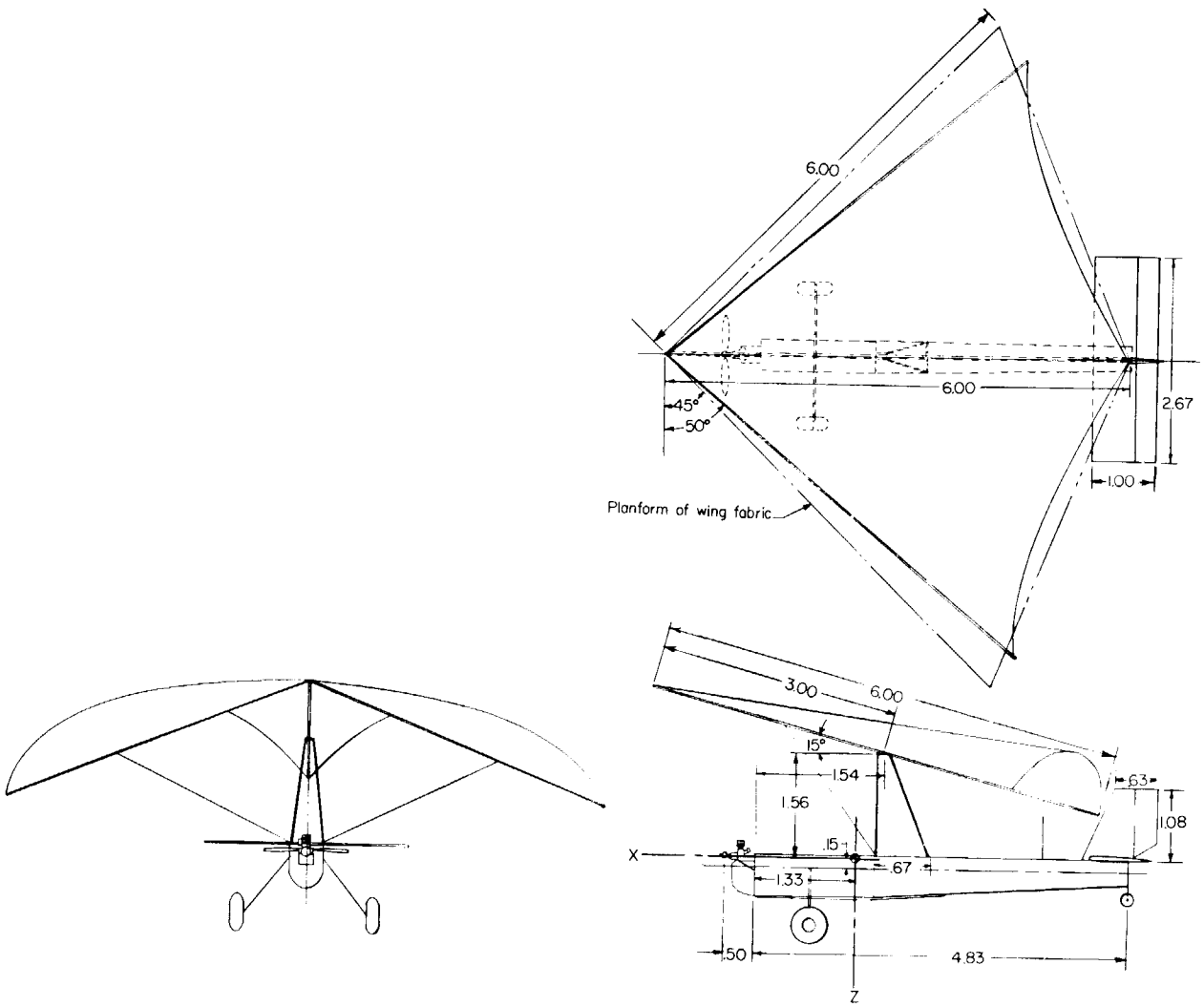

Figure 5.- Sketch of the radio-controlled airplane model. All linear dimensions are in feet.

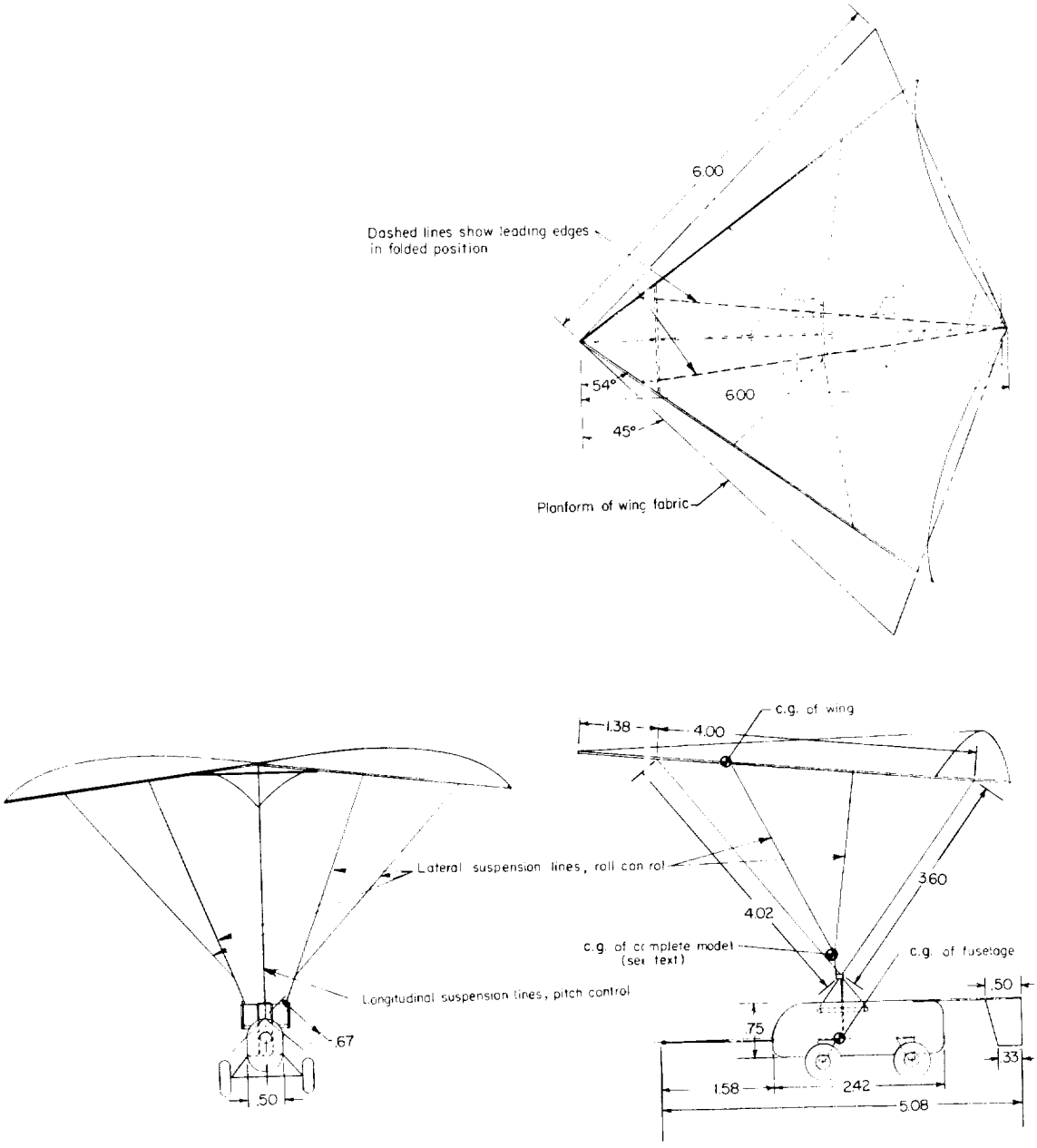

Figure 6.- Sketch of the modified radio-controlled glider model. All linear dimensions are in feet.

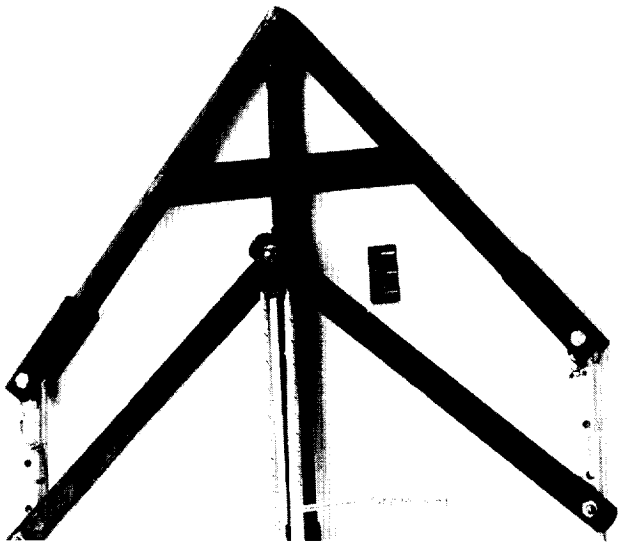

(a) Foldable nose in the folded position.

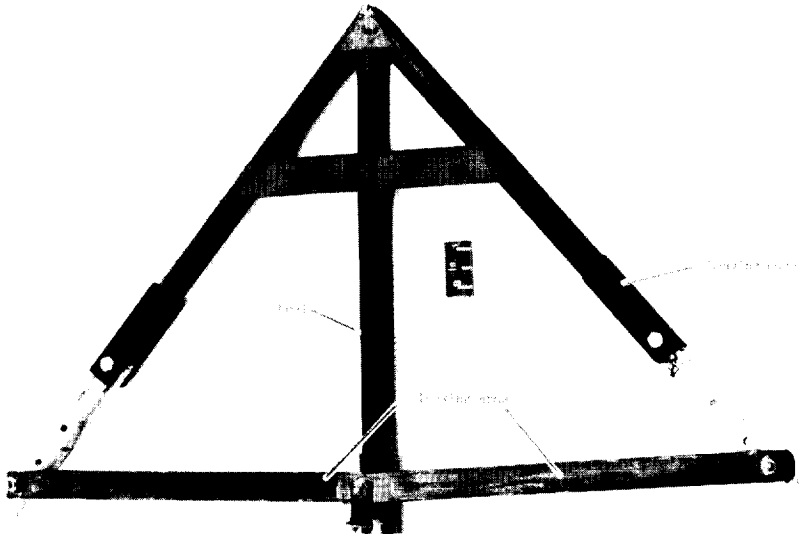

(b) Foldable nose in the extended position. L-61-2202

Figure 7.- Nose assembly for the parawing glider model with the fabric removed.

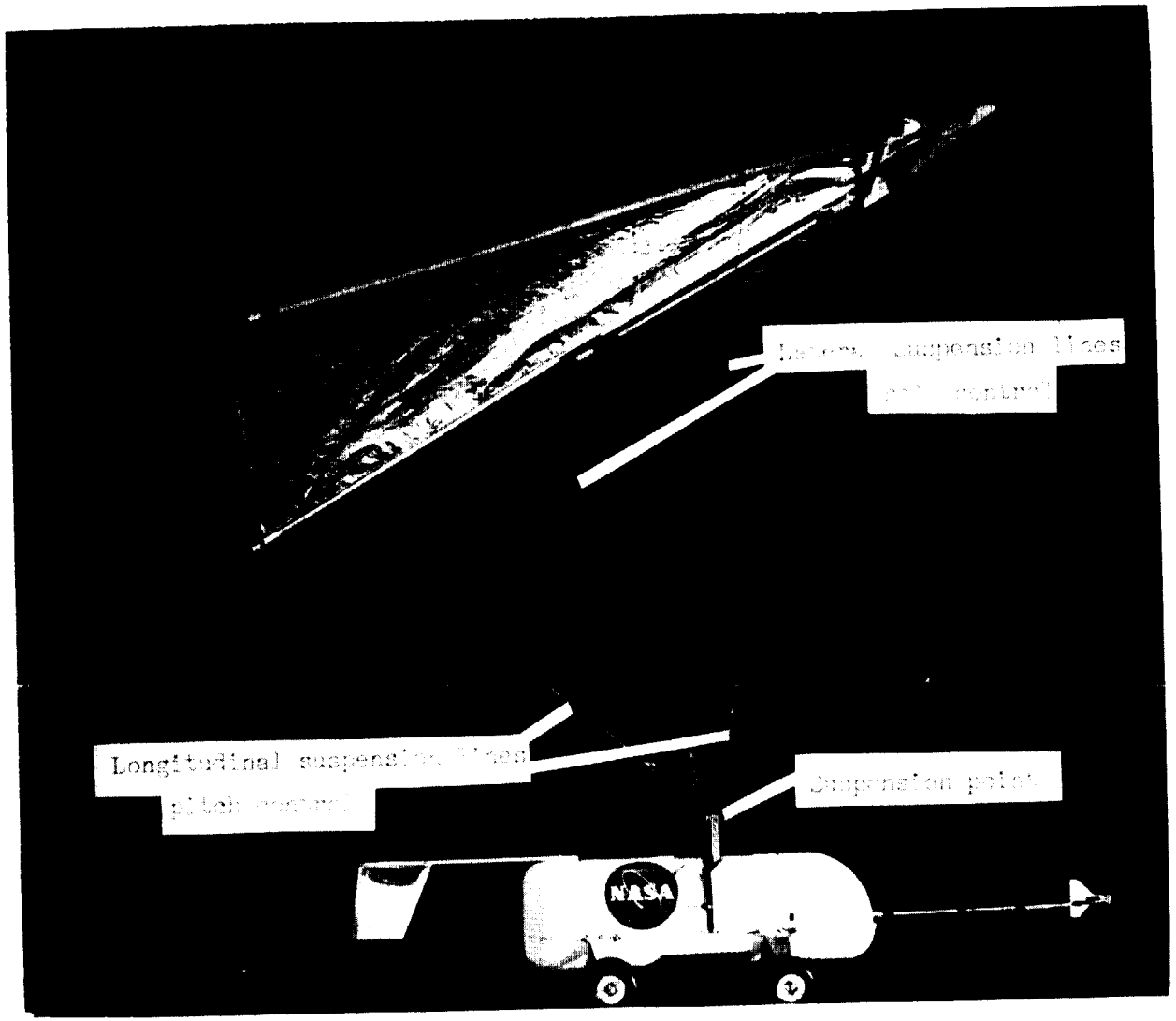

Figure 8.- Modified radio-controlled glider model. L-60-7461.1

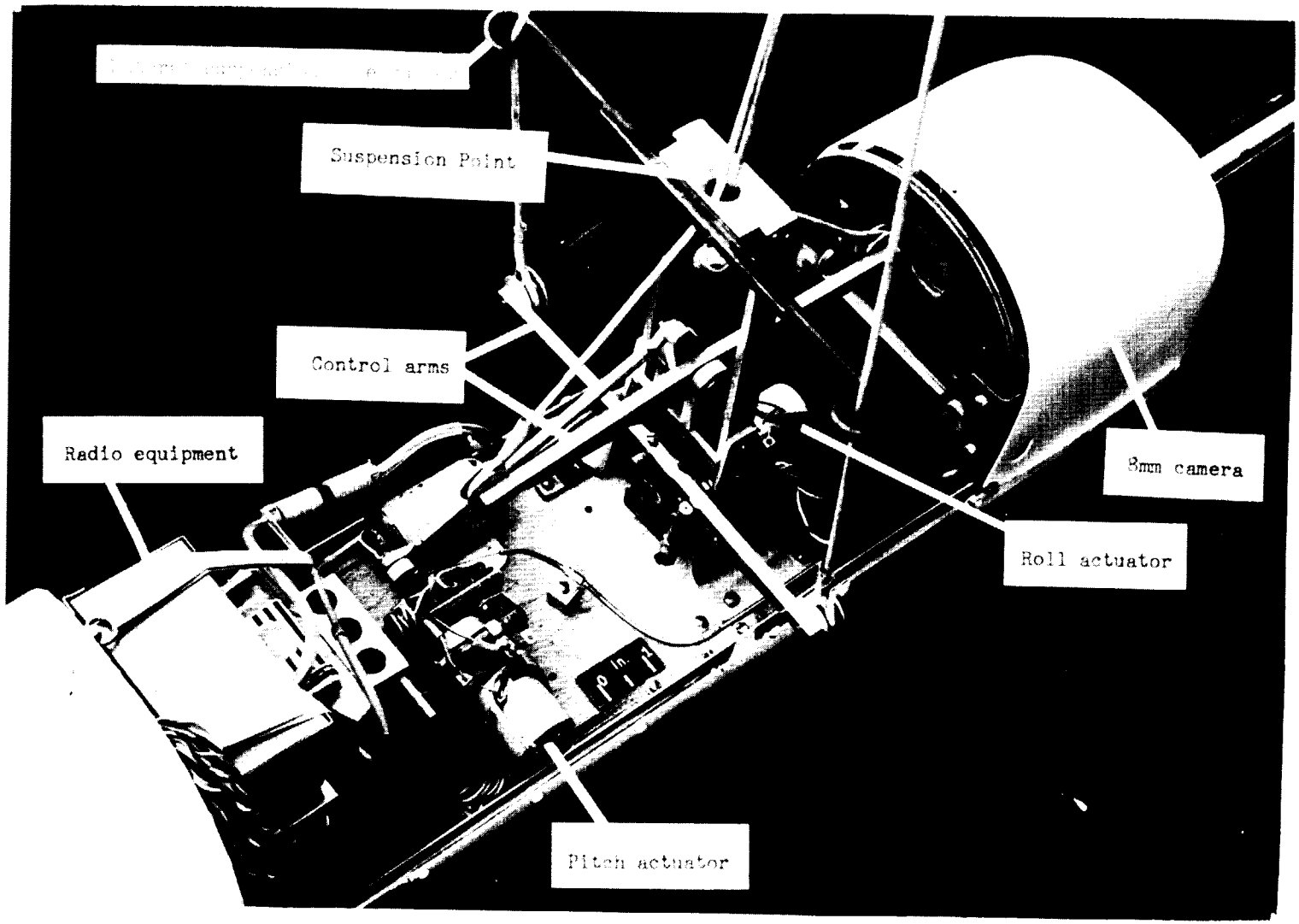

Figure 9.- Details of the control system of the modified glider model. L-60-5963.1

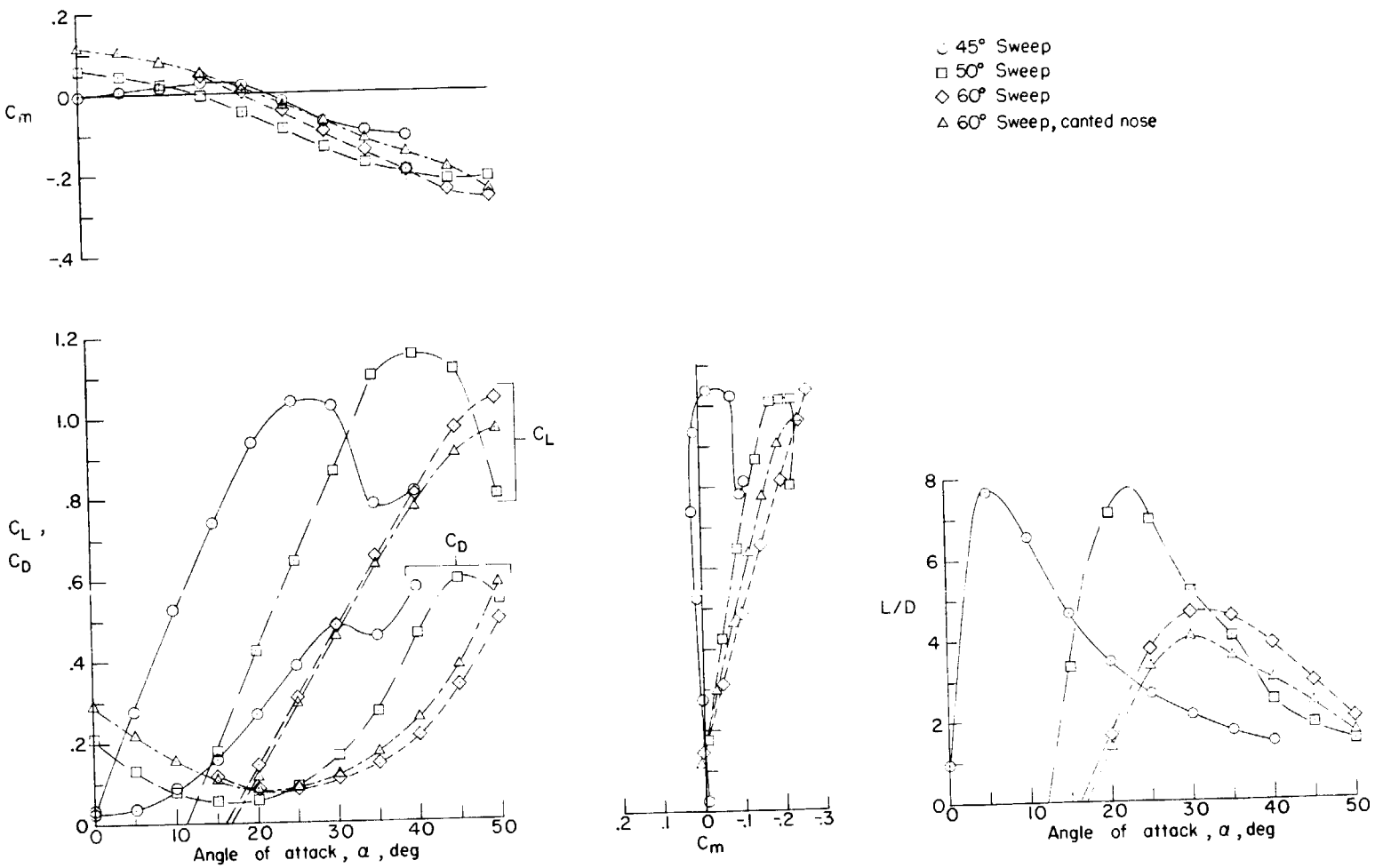

Figure 10.- Variations of C_L, C_D, C_m, and L/D with α, and C_L and C_D with C_m of the rigid wing for three angles of sweepback.

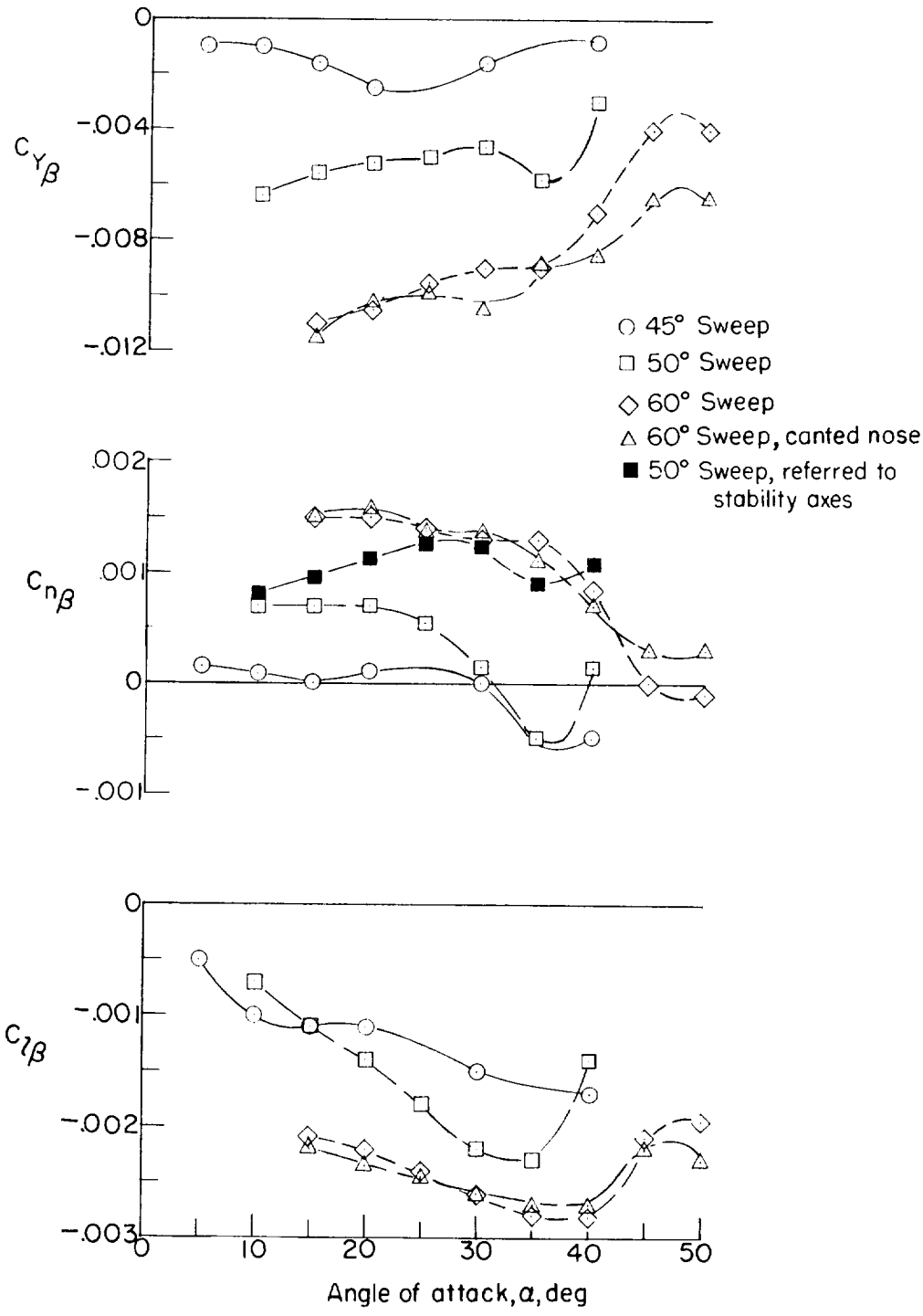

Figure 11.- Variations of the lateral stability parameters of the rigid wing with angle of attack for three angles of sweepback.

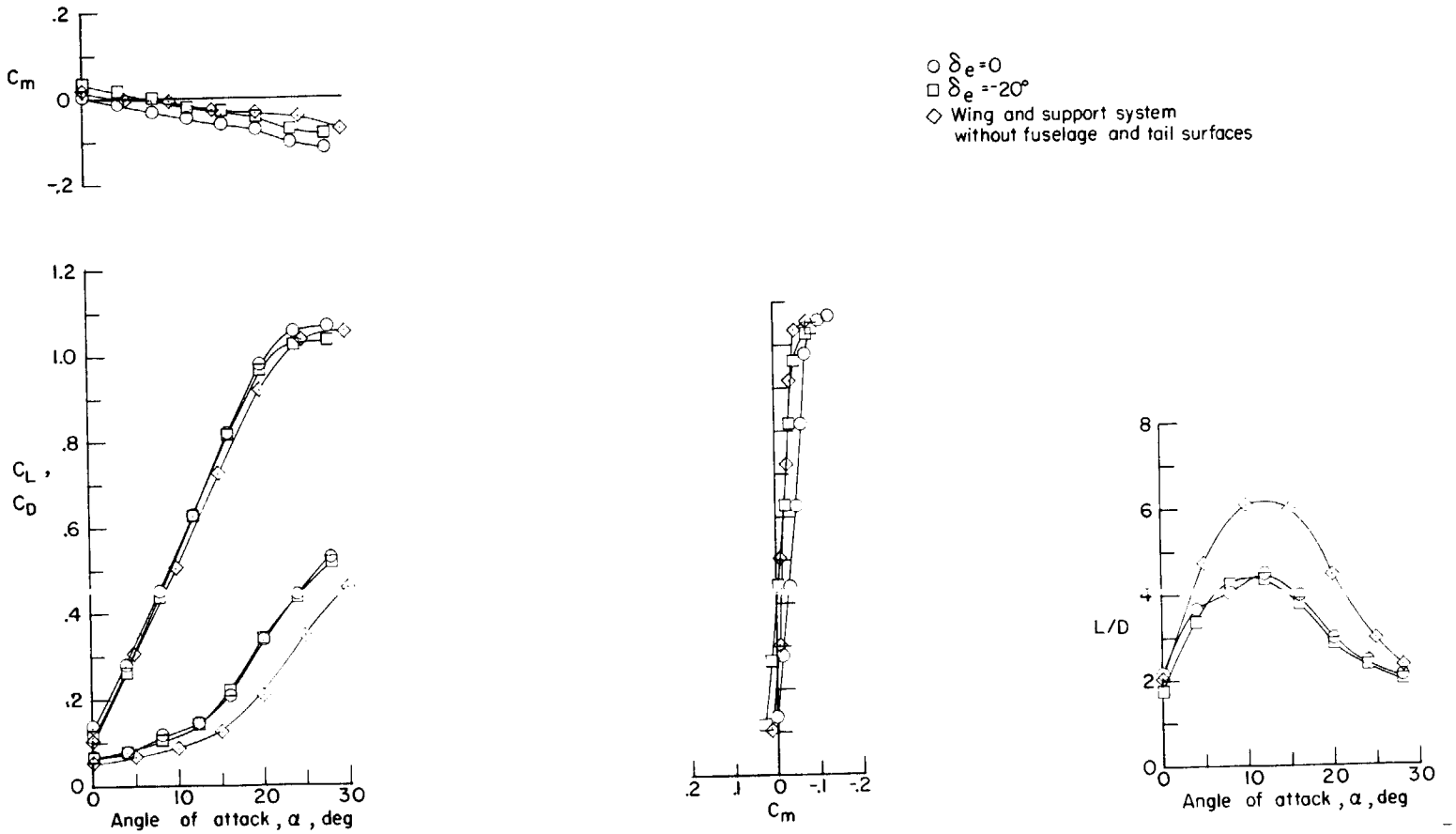

Figure 12.- Variations of C_L, C_D, C_m and L/D of the airplane model with α and C_L and C_D with C_m for two elevator deflections.

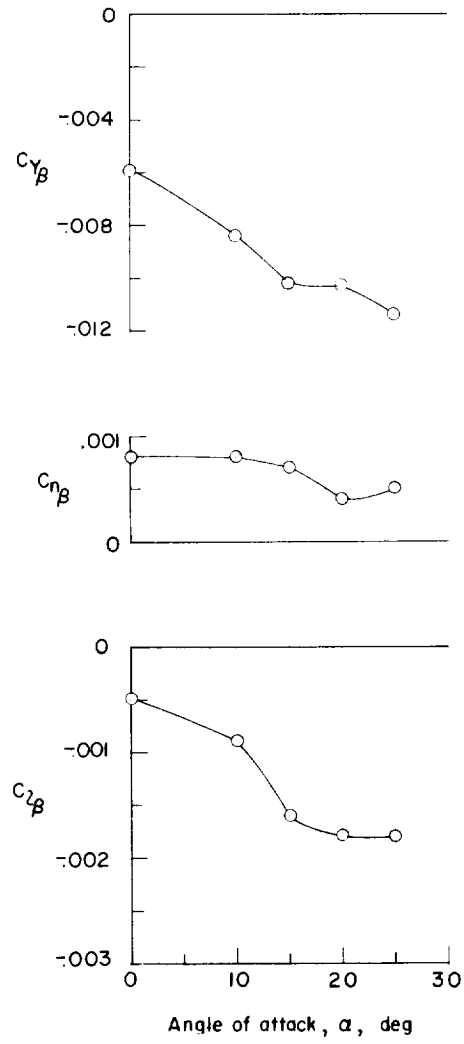

Figure 13.- Variations of the lateral stability parameters of the airplane model with angle of attack.

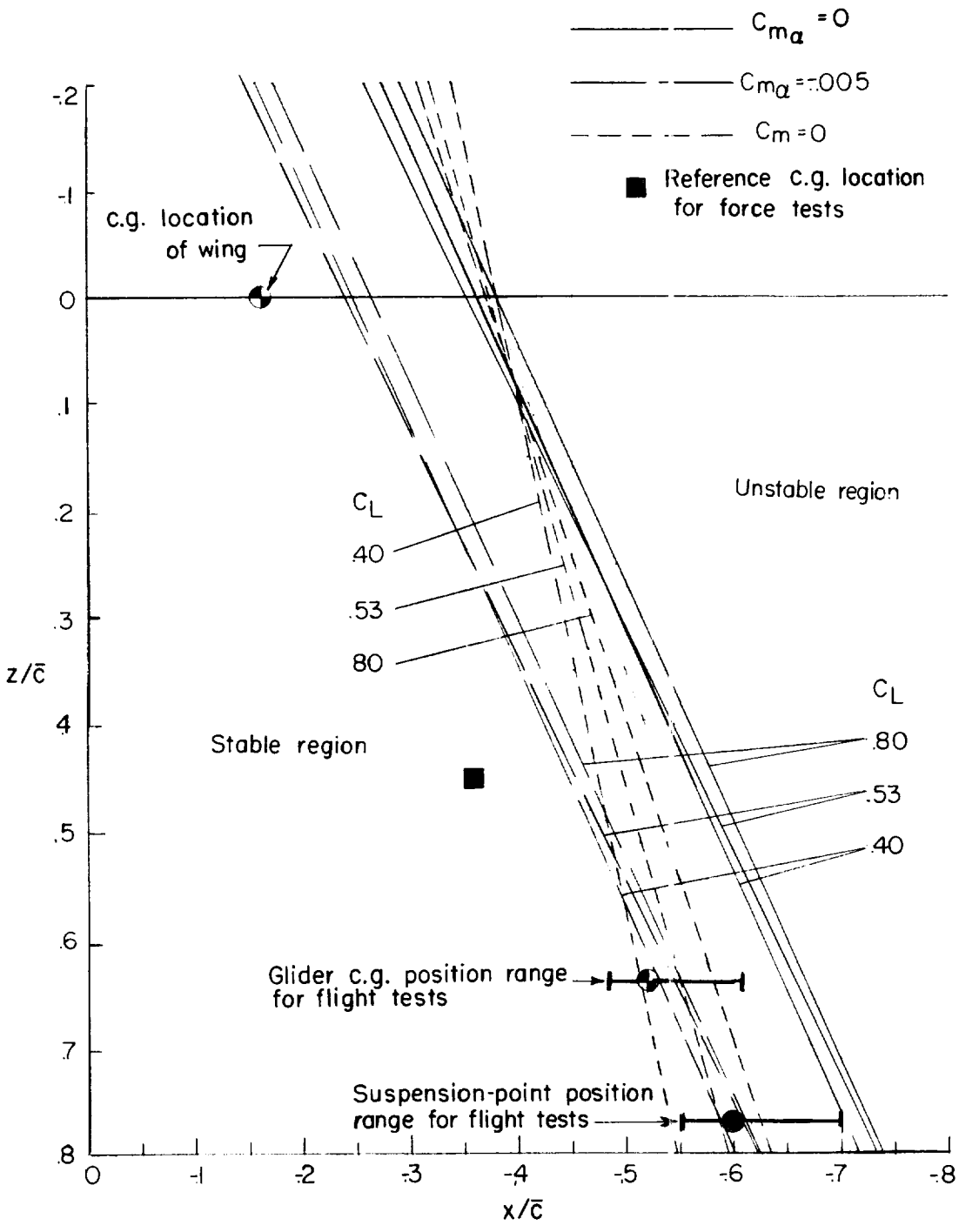

Figure 14.- Effect of center-of-gravity location on trimmed lift coefficient and static longitudinal stability for the glider model.

L-1374